Supplementary Information

Design and development of salen-type Schiff bases as potential antivirus agents: Experimental and theoretical approach

Sunil Kumar & Mukesh Choudhary*

Department of Chemistry, National Institute of Technology Patna, Patna 800 005, Bihar, India

*E-mail: mukesh@nitp.ac.in

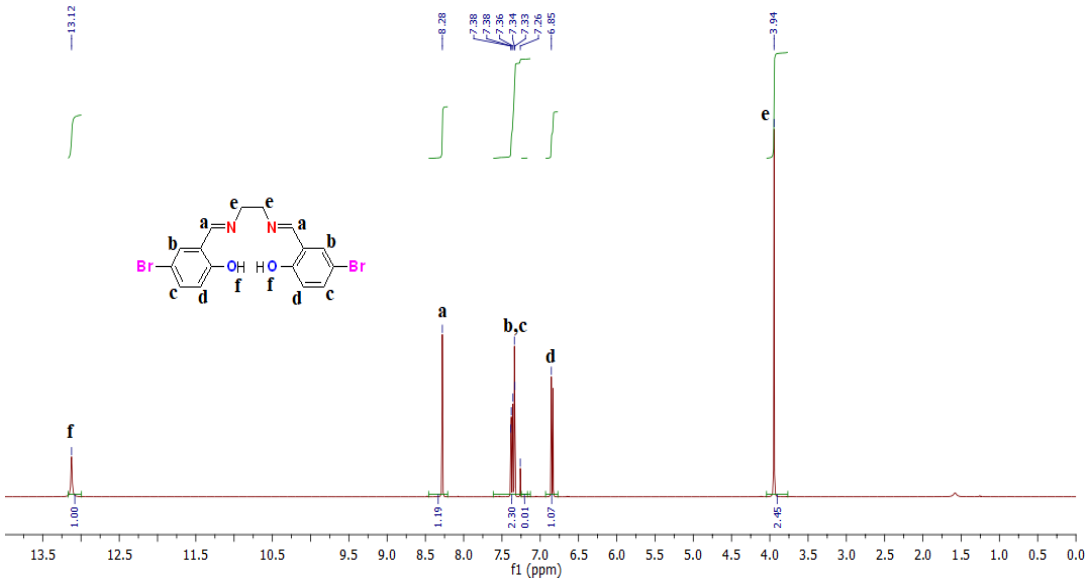

Fig. S1 — ^{1}H-NMR spectrum of salen-type compound LH_2

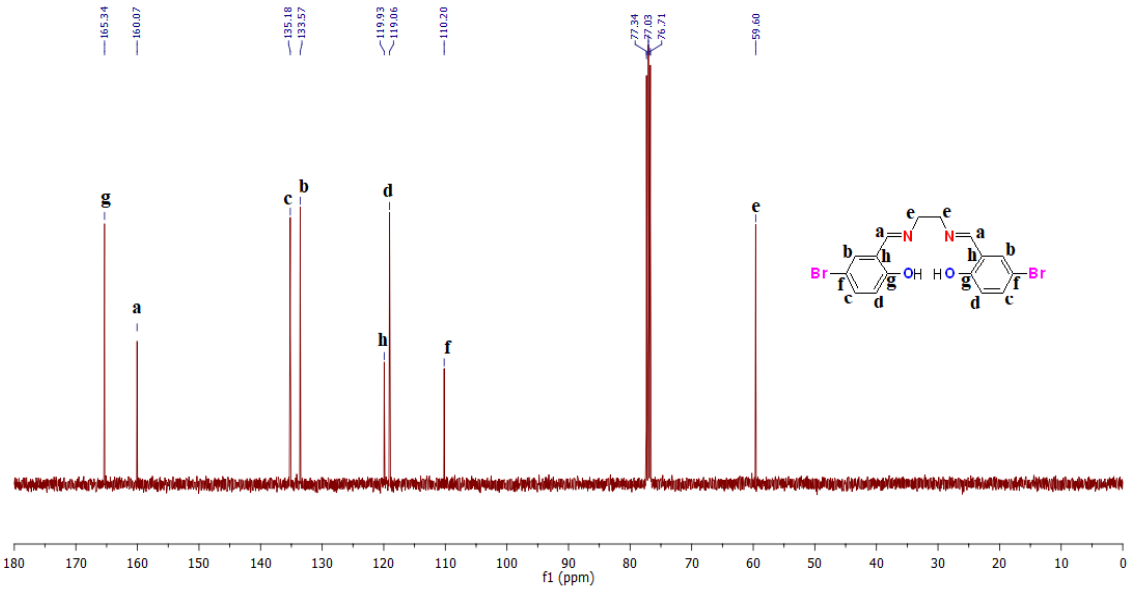

Fig. S2 — ^{13}C-NMR spectrum of the salen-type compound LH_2

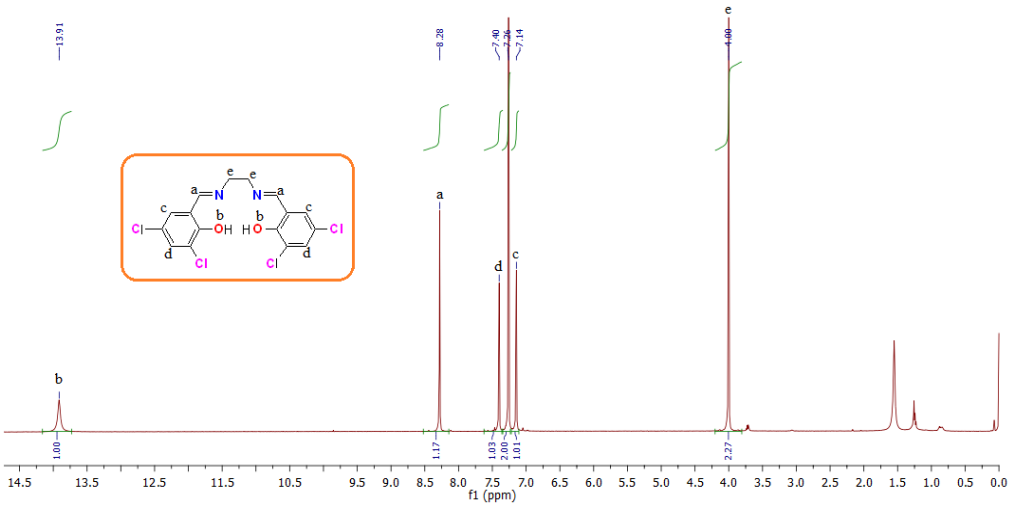

Fig. S3 — ^{1}H-NMR spectrum of the salen-type compound $L^{1}H_{2}$

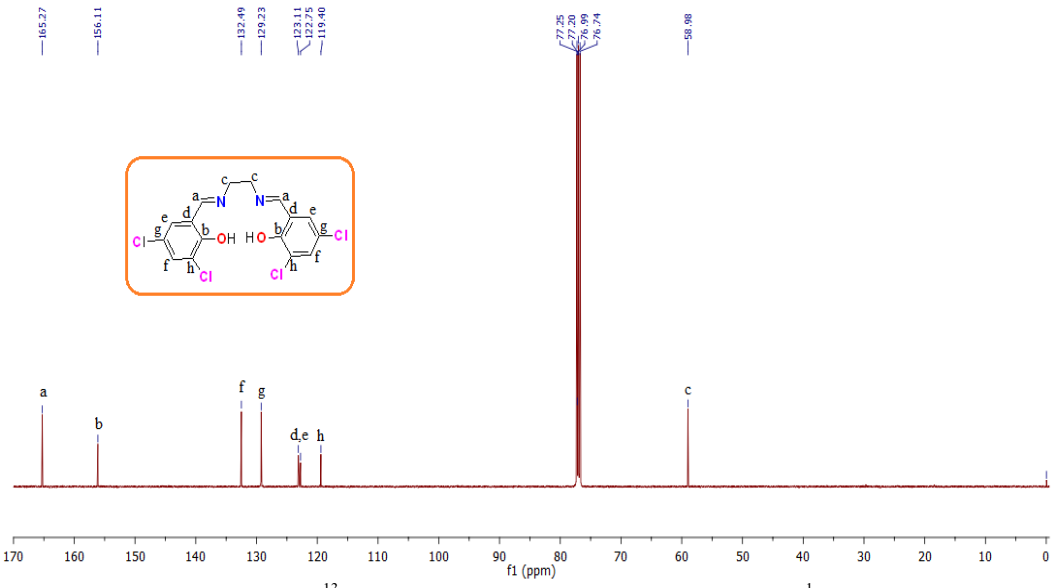

Fig. S4 — ^{13}C-NMR spectrum of the salen-type compound $L^{1}H_{2}$

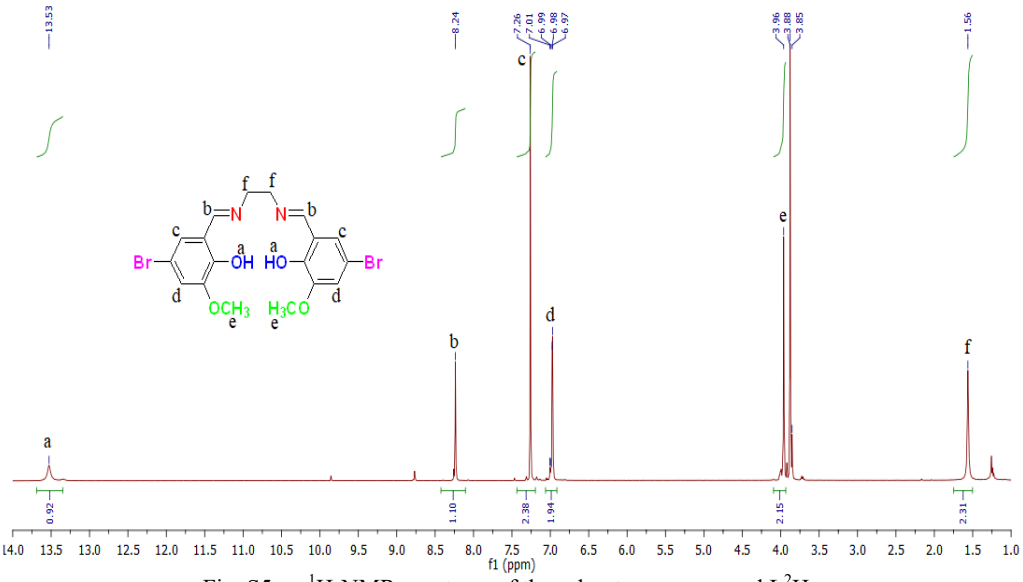

Fig. S5 — ^{1}H-NMR spectrum of the salen-type compound $L^{2}H_{2}$

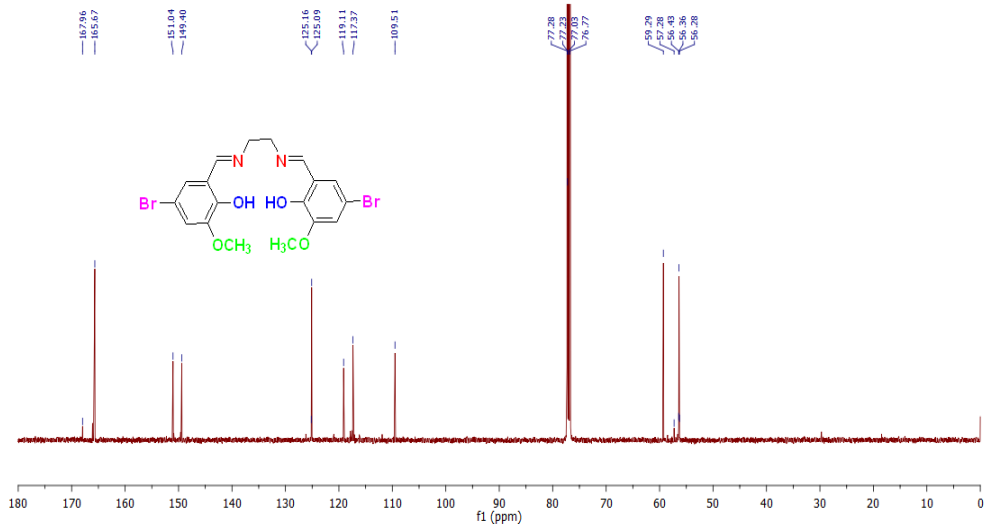

Fig. S6 — ^{13}C-NMR spectrum of the salen-type compound $L^{2}H_{2}$

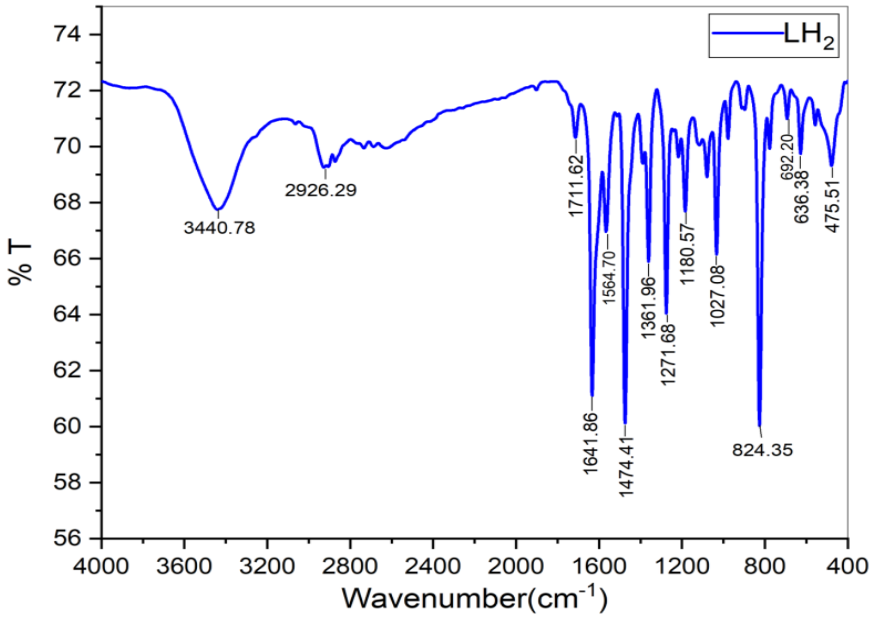

Fig. S7 — FT-IR spectrum of salen-type compound LH_2

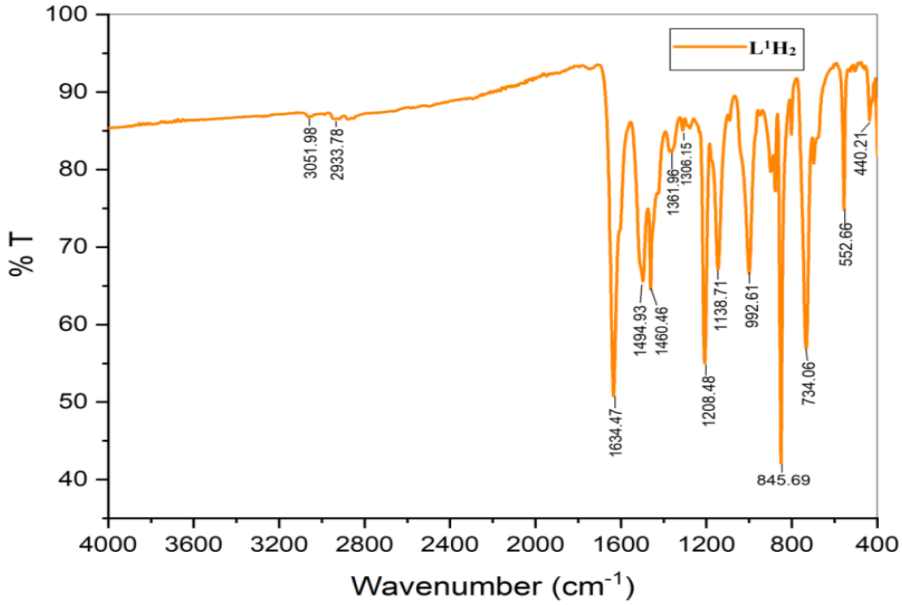

Fig. S8 — FT-IR spectrum of salen-type compound L^1H_2

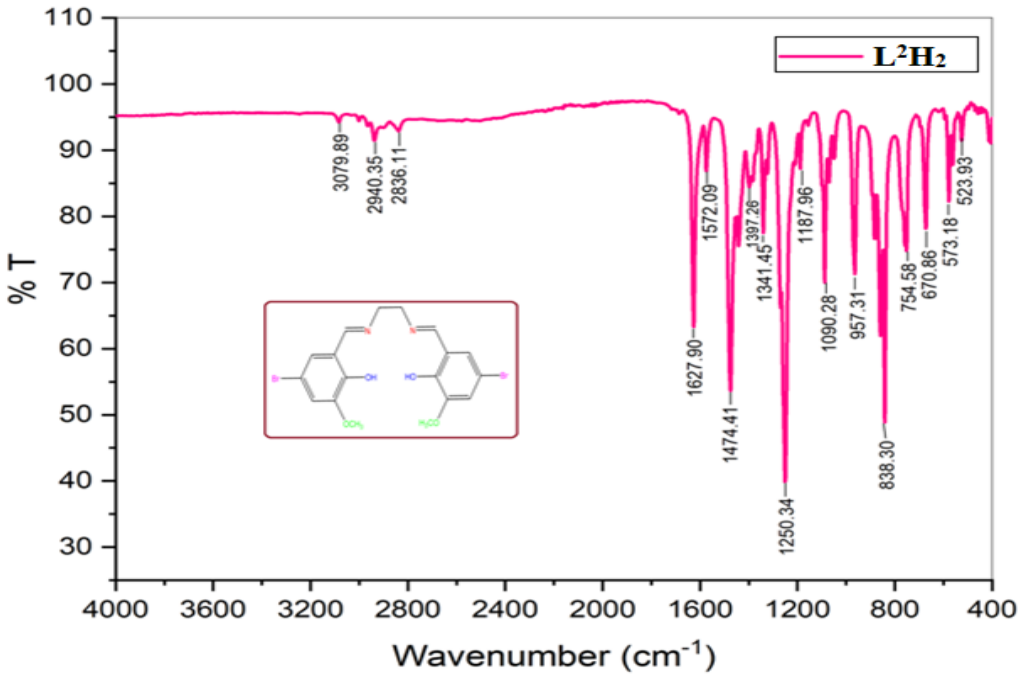

Fig. S9 — FT-IR spectrum of salen-type compound L^2H_2

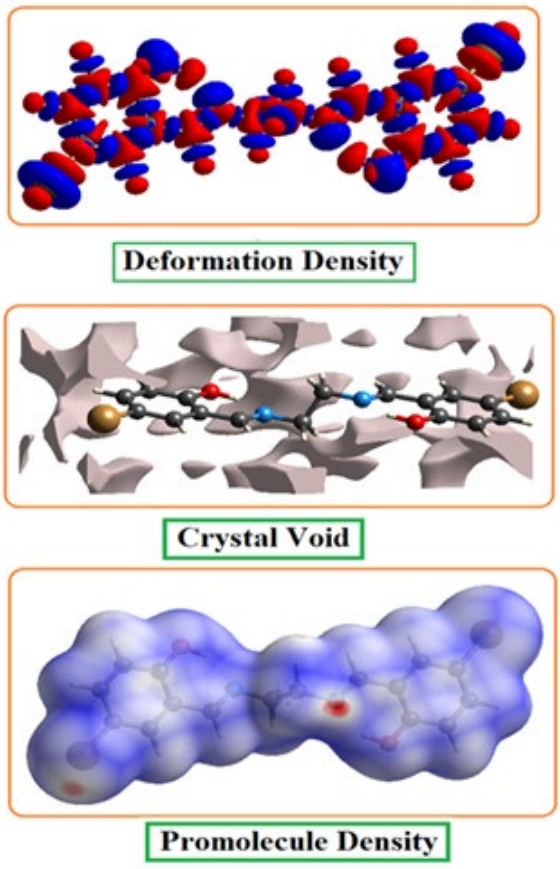

Fig. S10 — Deformation density, crystal void and promolecular density of the salen-type compound LH_2

	N	Symop	R	Electron Density	E_ele	E_pol	E_dis	E_rep	E_tot
	2	x, y, z	18.74	HF/3-21G	4.8	-0.2	-7.8	0.0	-2.3
	2	x, y, z	18.09	HF/3-21G	-3.2	-0.1	-5.1	0.0	-7.9
	4	-x, y+1/2, -z+1/2	4.70	HF/3-21G	-9.2	-6.5	-70.2	34.7	-48.7
	2	x, y, z	6.11	HF/3-21G	-24.8	-6.0	-36.0	13.6	-50.6

Energy Model	k_ele	k_pol	k_disp	k_rep
CE-HF ... HF/3-21G electron densities	1.019	0.651	0.901	0.811
CE-B3LYP ... B3LYP/6-31G(d,p) electron densities	1.057	0.740	0.871	0.618

Fig. S11 — CE-B3LYP estimates of energy components and total energies (kJ/mol) for the closest intermolecular interactions in the salen-type compound LH_2

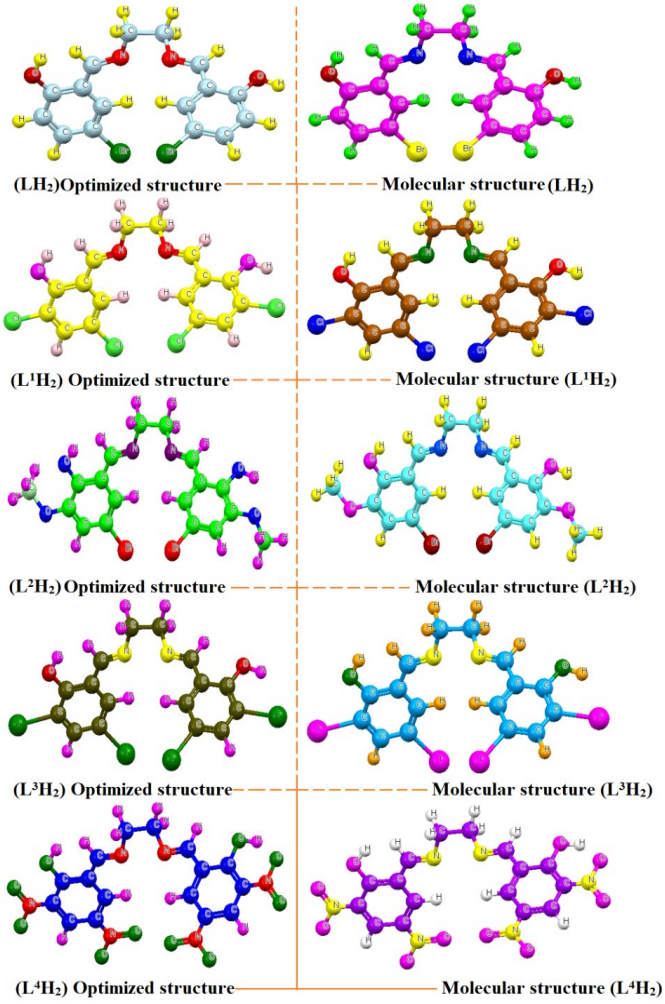

Fig. S12 — Optimized and molecular structures of salen-type compoundsLH_2- L^4H_2

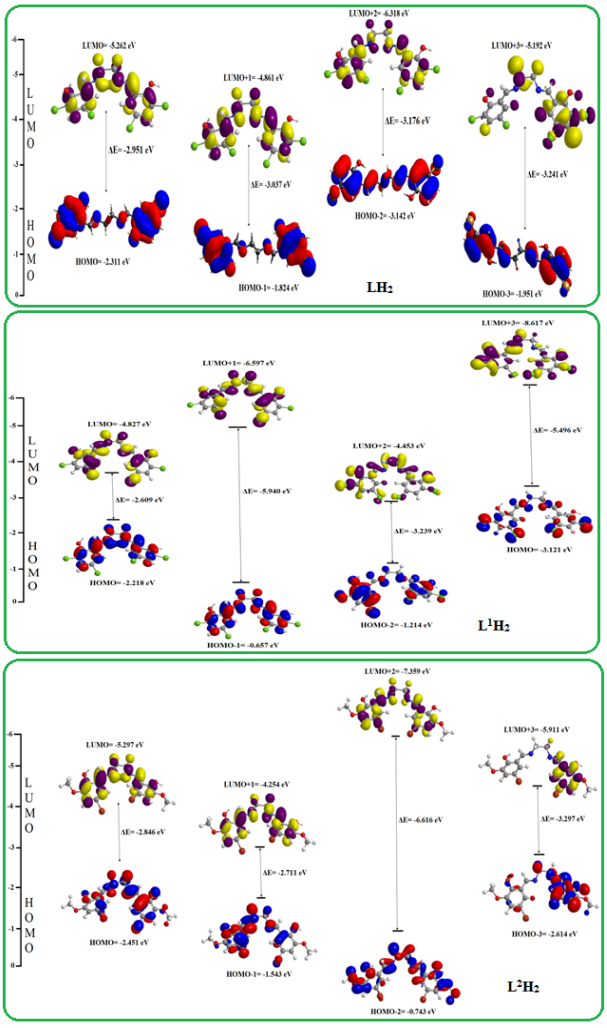

Fig. S13 — HOMO-LUMO energies and energy gap of salen-type compounds LH_2, L^1H_2 and L^2H_2

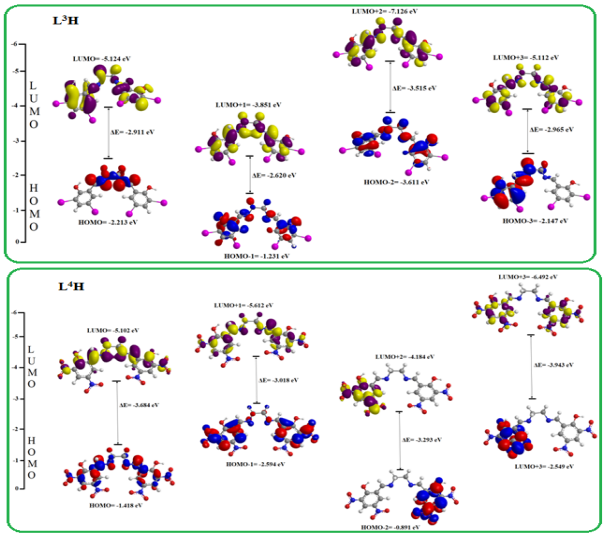

Fig. S14 — HOMO-LUMO energies and energy gap of salen-type compounds L^1H_2 and L^2H_2

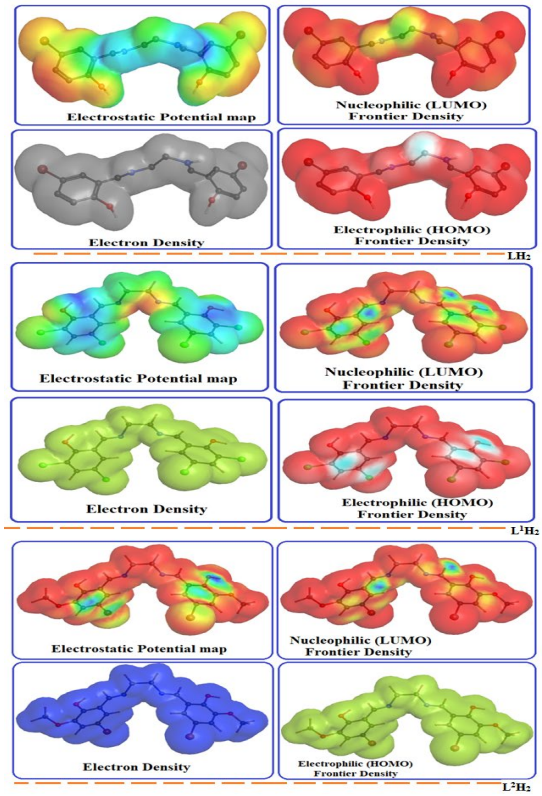

Fig. S15 — MEPs presentation including (a) radical frontier density, (b) electrophilic and nucleophilic frontier density (c) surface density forsalen-type compounds LH_2, L^1H_2 and L^2H_2

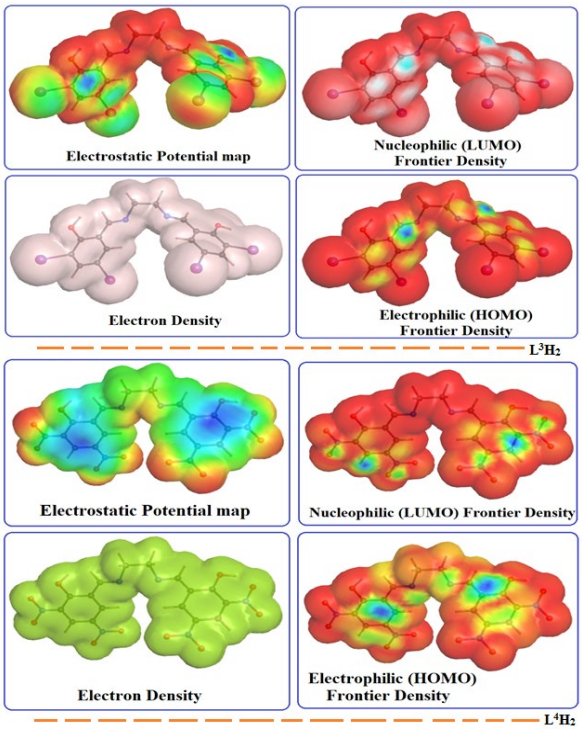

Fig. S16 — MEPs presentation including (a) radical frontier density, (b) electrophilic and nucleophilic frontier density (c) surface density for salen-type compounds L^3H_2 and L^4H_2

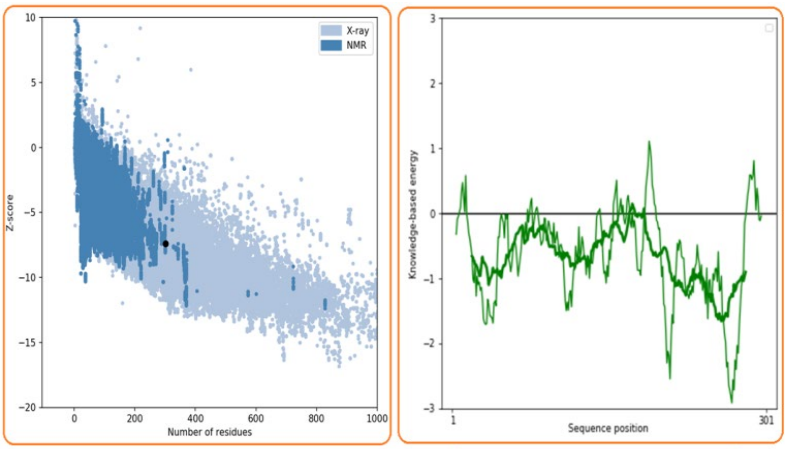

Fig. S17 — Graphical view of overall model quality and residue scores of SARS-CoV-2 main protease (PDB ID: 7O46)

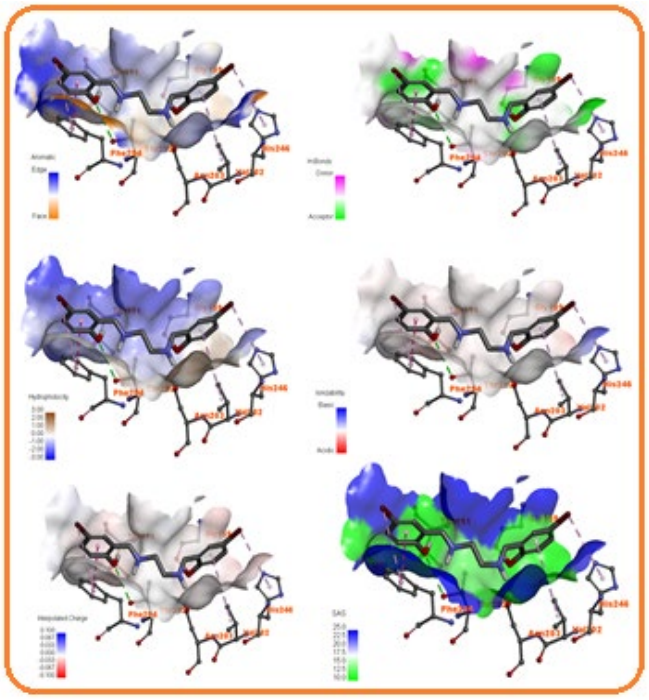

Fig. S18 — The representation of docked LH_2 compound with SARS-CoV-2 main protease for COVID-19 (PDB ID: 7O46) with its focused view for interacting residues along with H-bond and intermolecular interactions; (a) Aromatic receptor surface represented by blue (Edge) and light orange (face) colours; (b) H-bond donor and acceptor meshes represented by pink and light green colours, respectively; (c) Hydrophobic pocket represented with blue and brown colours; (d) Ionizability receptor surface represented by blue (basic) and red (acidic) colours (e) interpolated charge receptor surface represented by blue and red colours; (f) SAS receptor surface represented by blue and light green colours, respectively

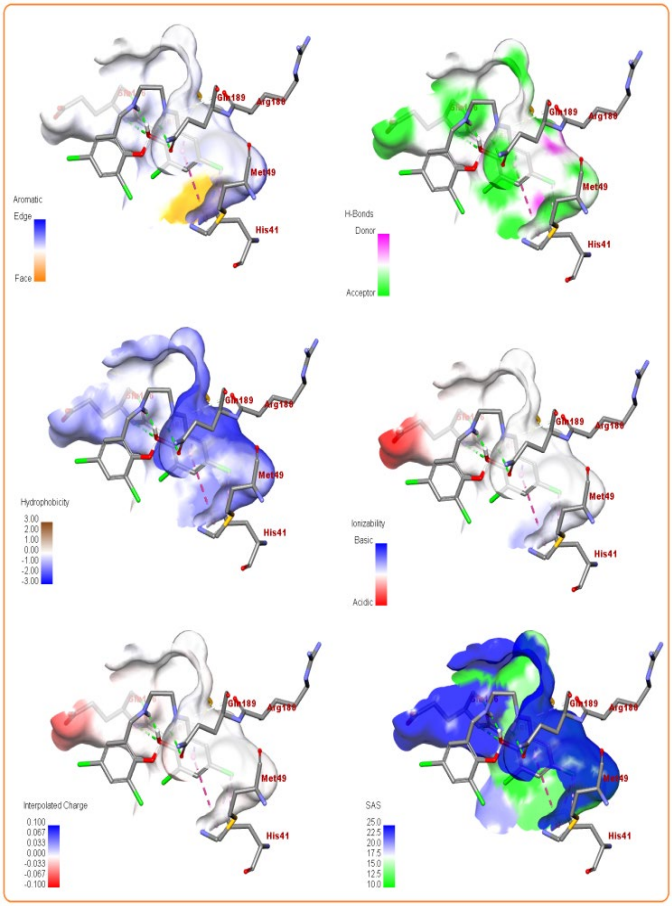

Fig. S19 — The representation of docked L^1H_2 compound with SARS-CoV-2 main protease for COVID-19 (PDB ID: 7O46) with its focused view for interacting residues along with H-bond and intermolecular interactions; (a) Aromatic receptor surface represented by blue (Edge) and light orange (face) colours; (b) H-bond donor and acceptor meshes represented by pink and light green colours, respectively; (c) Hydrophobic pocket represented with blue and brown colours; (d) Ionizability receptor surface represented by blue (basic) and red (acidic) colours (e) interpolated charge receptor surface represented by blue and red colours; (f) SAS receptor surface represented by blue and light green colours, respectively

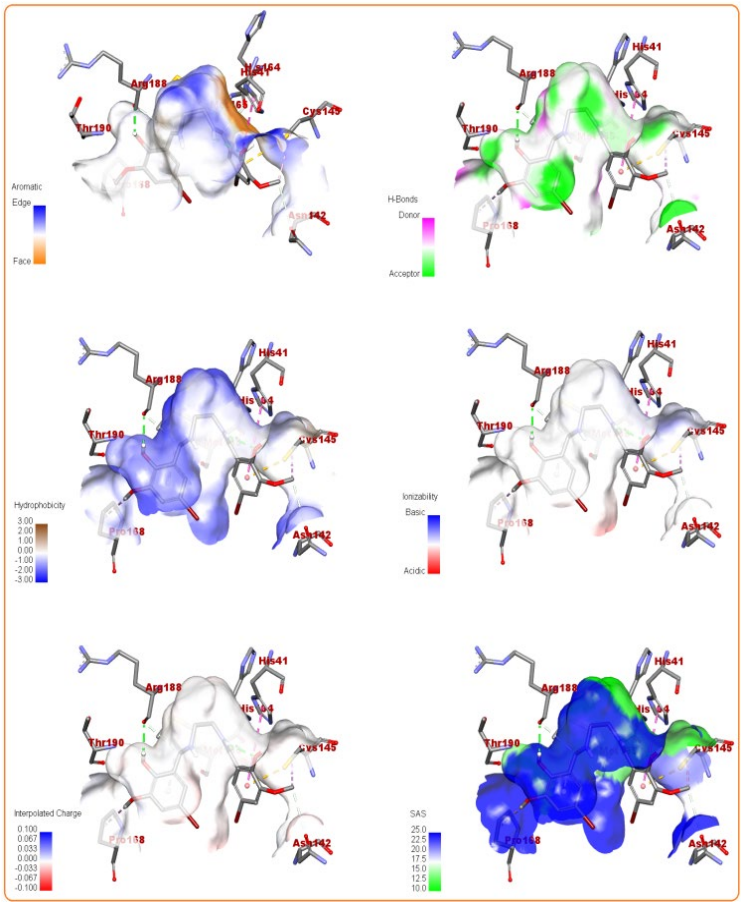

Fig. S20 — The representation of docked L^2H_2compound with SARS-CoV-2 main protease for COVID-19 (PDB ID: 7O46) with its focused view for interacting residues along with H-bond and intermolecular interactions; (a) Aromatic receptor surface represented by blue (Edge) and light orange (face) colours; (b) H-bond donor and acceptor meshes represented by pink and light green colours, respectively; (c) Hydrophobic pocket represented with blue and brown colours; (d) Ionizability receptor surface represented by blue (basic) and red (acidic) colours (e) Interpolated charge receptor surface represented by blue and red colours; (f) SAS receptor surface represented by blue and light green colours, respectively

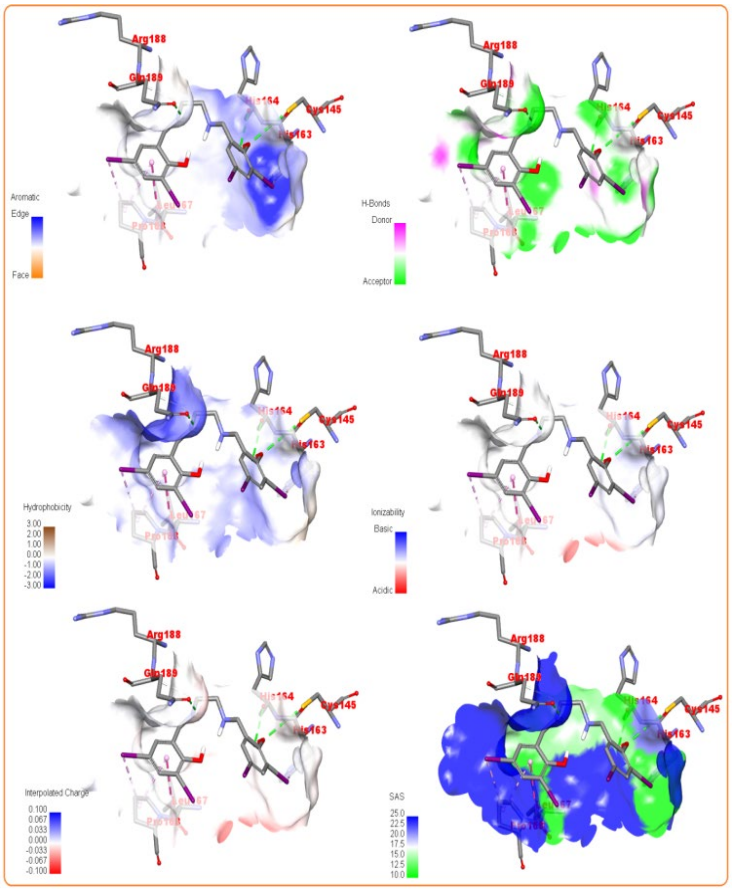

Fig. S21 — The representation of docked L^3H_2compound with SARS-CoV-2 main protease for COVID-19 (PDB ID: 7O46) with its focused view for interacting residues along with H-bond and intermolecular interactions; (a) Aromatic receptor surface represented by blue (Edge) and light orange (face) colours; (b) H-bond donor and acceptor meshes represented by pink and light green colours, respectively; (c) Hydrophobic pocket represented with blue and brown colours; (d) Ionizability receptor surface represented by blue (basic) and red (acidic) colours (e) Interpolated charge receptor surface represented by blue and red colours; (f) SAS receptor surface represented by blue and light green colours

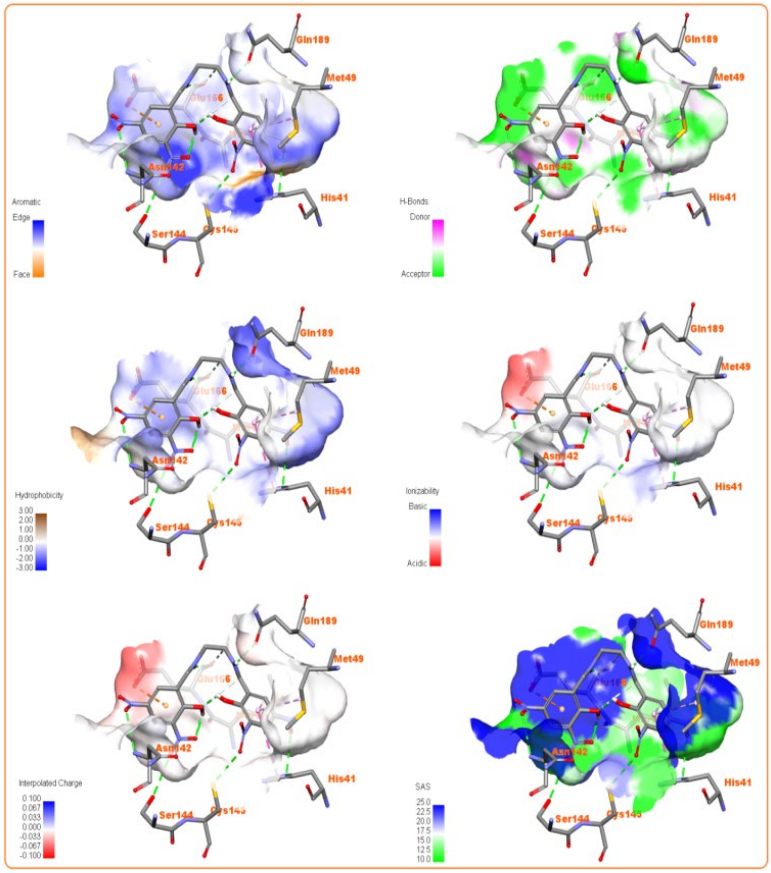

Fig. S22 — The representation of docked L^4H_2compound with SARS-CoV-2 main protease for COVID-19 (PDB ID: 7O46) with its focused view for interacting residues along with H-bond and intermolecular interactions; (a) Aromatic receptor surface represented by blue (Edge) and light orange (face) colours; (b) H-bond donor and acceptor meshes represented by pink and light green colours, respectively; (c) Hydrophobic pocket represented with blue and brown colours; (d) Ionizability receptor surface represented by blue (basic) and red (acidic) colours (e) Interpolated charge receptor surface represented by blue and red colours; (f) SAS receptor surface represented by blue and light green colours, respectively

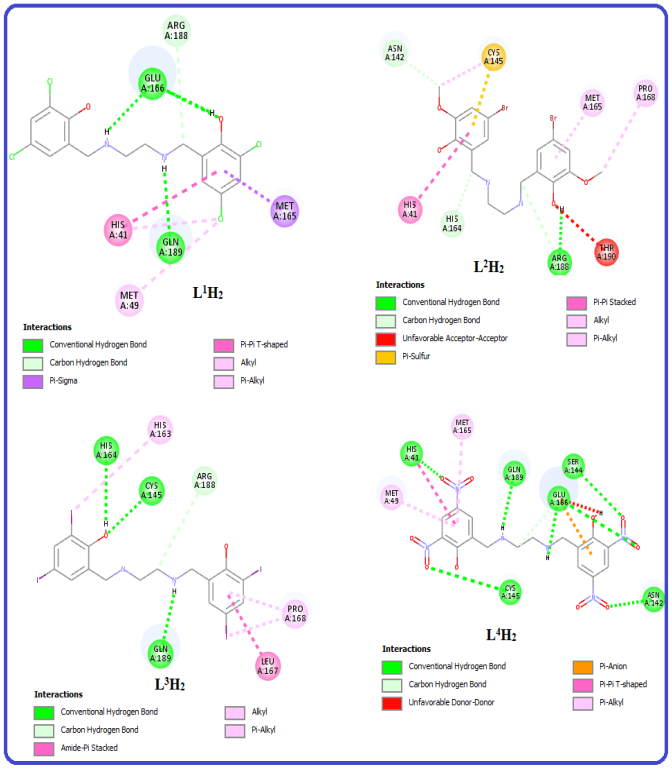

Fig. S23 — Two-dimensional diagrams of salen type compounds L^1H_2-L^4H_2 with SARS-CoV-2 main protease (M^{pro})

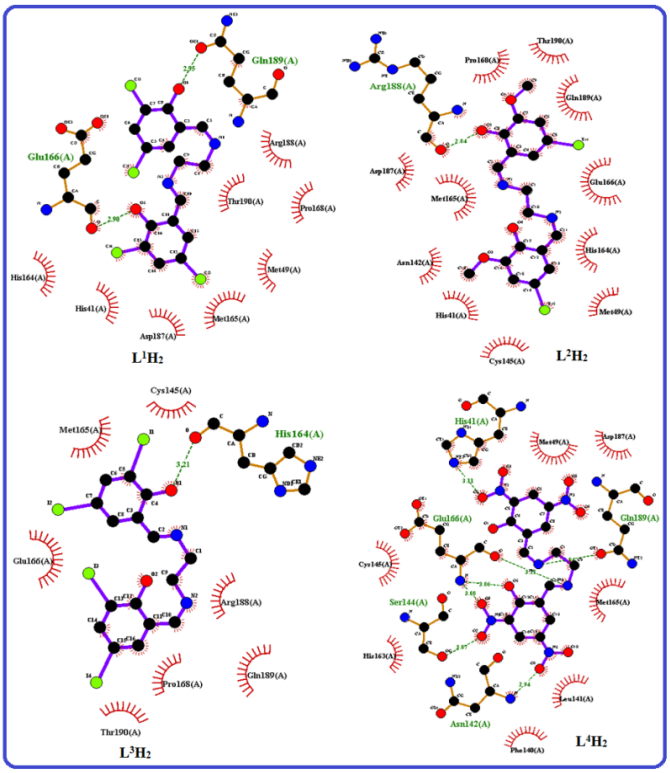

Fig. S24 — Two-dimensional Lig-plot image of salen type compounds L^1H_2-L^4H_2 with SARS-CoV-2 main protease (M^{pro})

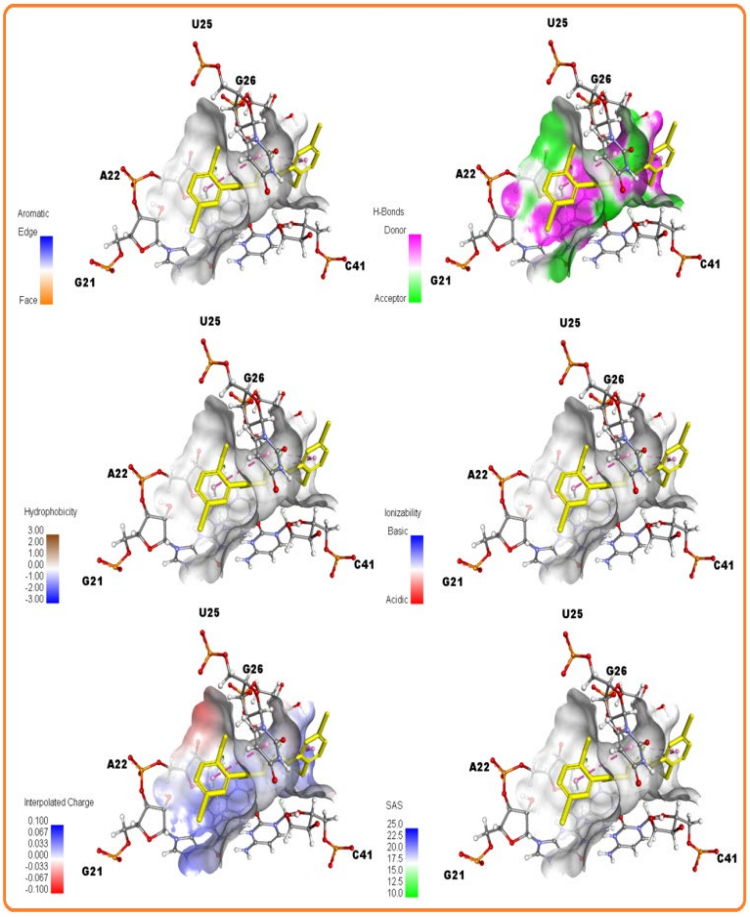

Fig. S25 — The representation of docked LH_2compound inside the HIV-1 virus (PDB ID: 1UUI) with its focused view for interacting nucleotide residues along with H-bond and intermolecular interactions; (a) H-bond donor and acceptor meshes represented by pink and light green colours, respectively; (a) Aromatic receptor surface represented by blue (Edge) and light orange (face) colours; (b) H-bond donor and acceptor meshes represented by pink and light green colours, respectively; (c) Hydrophobic pocket represented with blue and brown colours; (d) Ionizability receptor surface represented by blue (basic) and red (acidic) colours (e) Interpolated charge receptor surface represented by blue and red colours; (f) SAS receptor surface represented by blue and light green colours, respectively

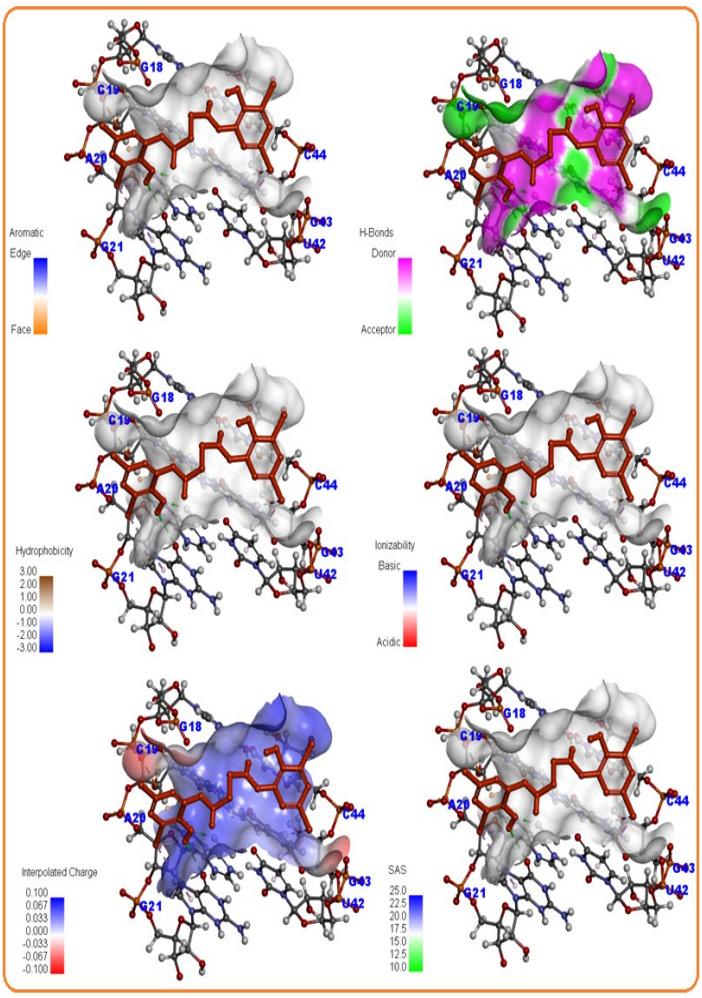

Fig. S26 — The representation of docked L^1H_2compound inside the HIV-1 virus (PDB ID: 1UUI) with its focused view for interacting nucleotide residues along with H-bond and intermolecular interactions; (a) Aromatic receptor surface represented by blue (Edge) and light orange (face) colours; (b) H-bond donor and acceptor meshes represented by pink and light green colours, respectively; (c) Hydrophobic pocket represented with blue and brown colours; (d) Ionizability receptor surface represented by blue (basic) and red (acidic) colours (e) Interpolated charge receptor surface represented by blue and red colours; (f) SAS receptor surface represented by blue and light green colours, respectively

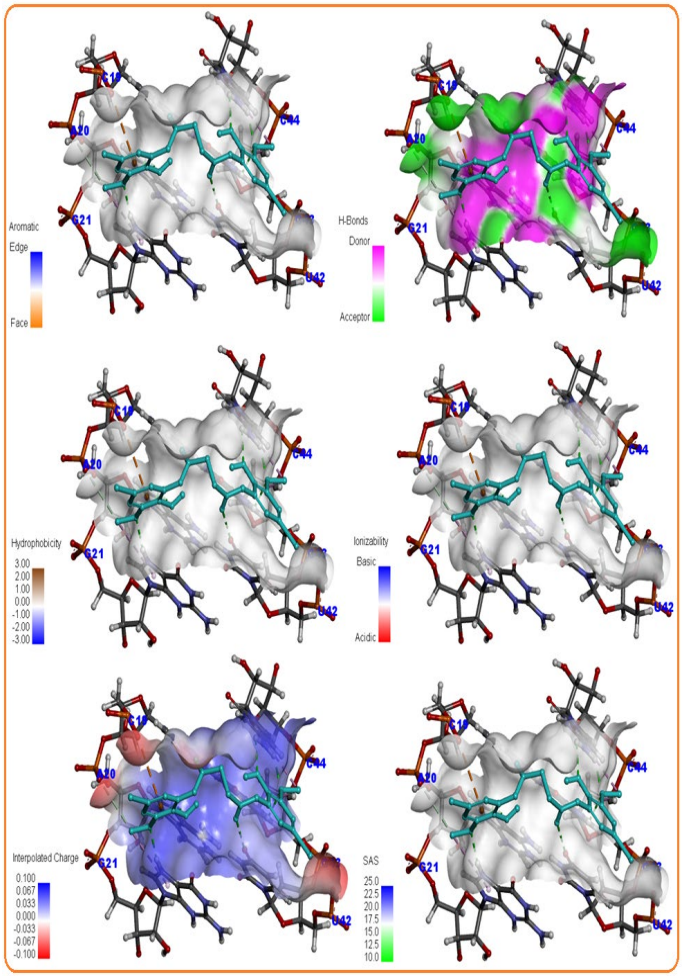

Fig. S27 — The representation of docked L2H2compound inside the HIV-1 virus (PDB ID: 1UUI) with its focused view for interacting nucleotide residues along with H-bond and intermolecular interactions; (a) Aromatic receptor surface represented by blue (Edge) and light orange (face) colours; (b) H-bond donor and acceptor meshes represented by pink and light green colours, respectively; (c) Hydrophobic pocket represented with blue and brown colours; (d) Ionizability receptor surface represented by blue (basic) and red (acidic) colours (e) Interpolated charge receptor surface represented by blue and red colours; (f) SAS receptor surface represented by blue and light green colours, respectively

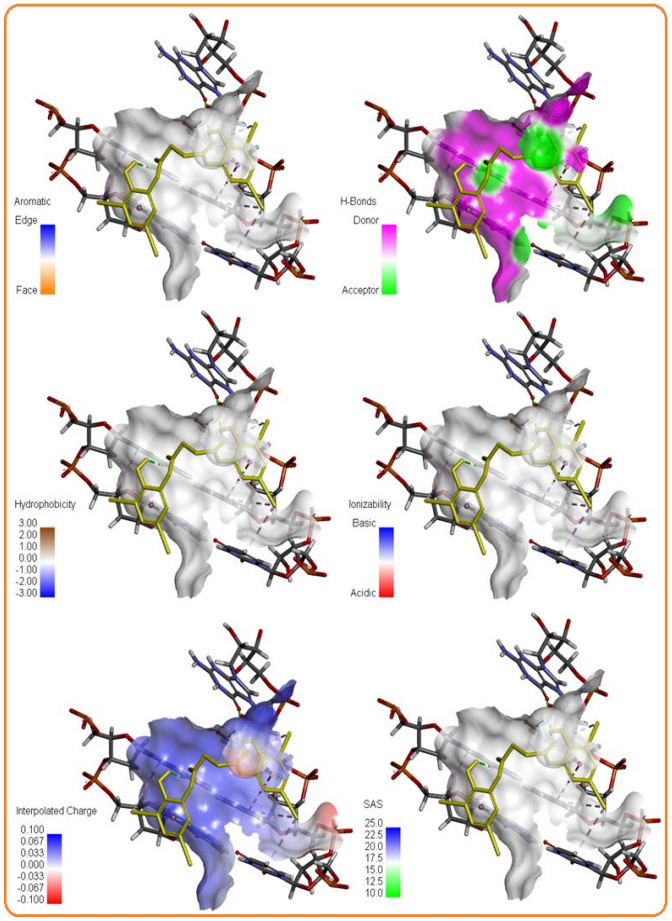

Fig. S28 — The representation of docked L^3H_2compound inside the HIV-1 virus (PDB ID: 1UUI) with its focused view for interacting nucleotide residues along with H-bond and intermolecular interactions; (a) Aromatic receptor surface represented by blue (Edge) and light orange (face) colours; (b) H-bond donor and acceptor meshes represented by pink and light green colours, respectively; (c) Hydrophobic pocket represented with blue and brown colours; (d) Ionizability receptor surface represented by blue (basic) and red (acidic) colours (e) Interpolated charge receptor surface represented by blue and red colours; (f) SAS receptor surface represented by blue and light green colours, respectively

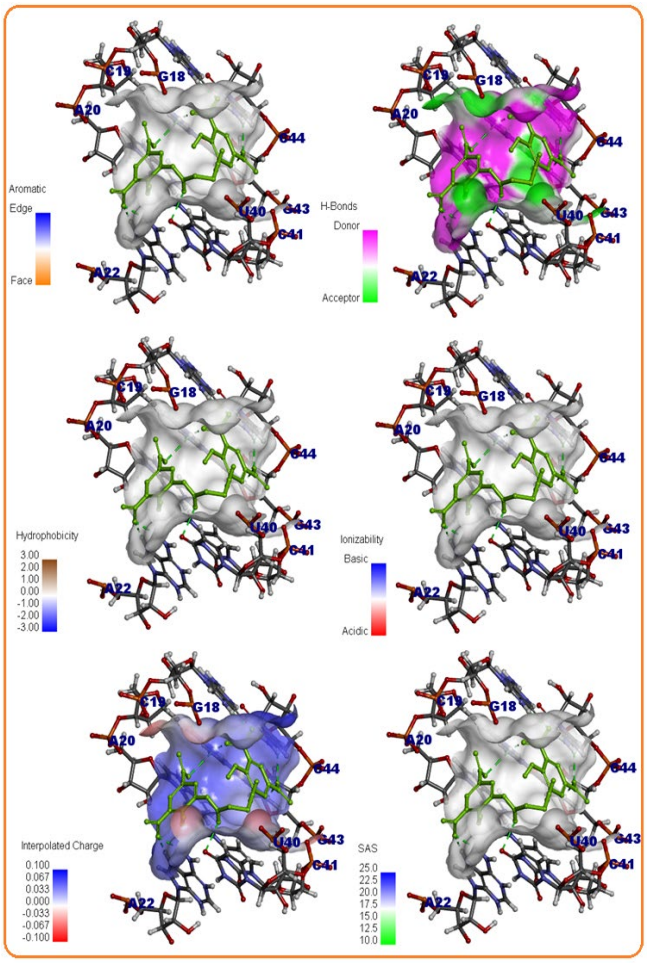

Fig. S29 — The representation of docked L^4H_2compound inside the HIV-1 virus (PDB ID: 1UUI) with its focused view for interacting nucleotide residues along with H-bond and intermolecular interactions; (a) Aromatic receptor surface represented by blue (Edge) and light orange (face) colours; (b) H-bond donor and acceptor meshes represented by pink and light green colours, respectively; (c) Hydrophobic pocket represented with blue and brown colours; (d) Ionizability receptor surface represented by blue (basic) and red (acidic) colours (e) Interpolated charge receptor surface represented by blue and red colours; (f) SAS receptor surface represented by blue and light green colours, respectively

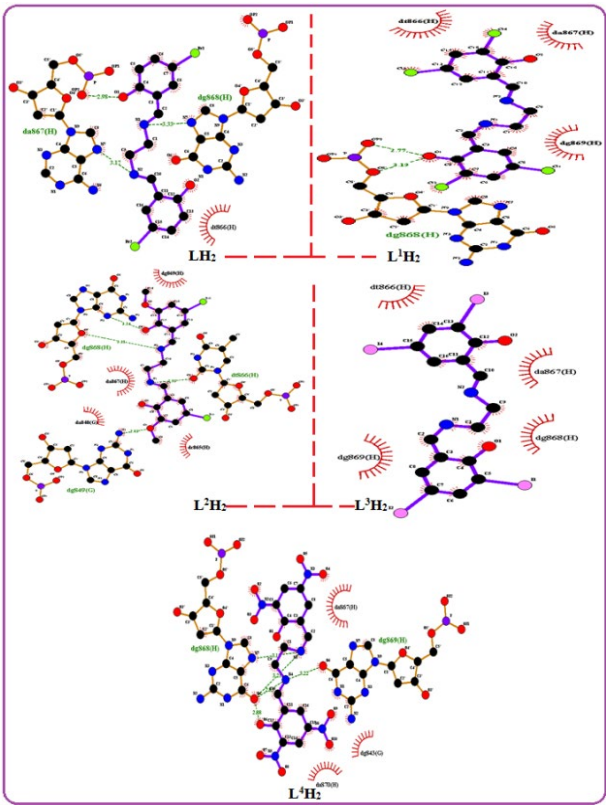

Fig. S30 — Two-dimensional interactions of docked ligands LH_2-L^4H_2 inside the DNA polymerase IV (PDB ID: 5YUX) generated by Lig Plot

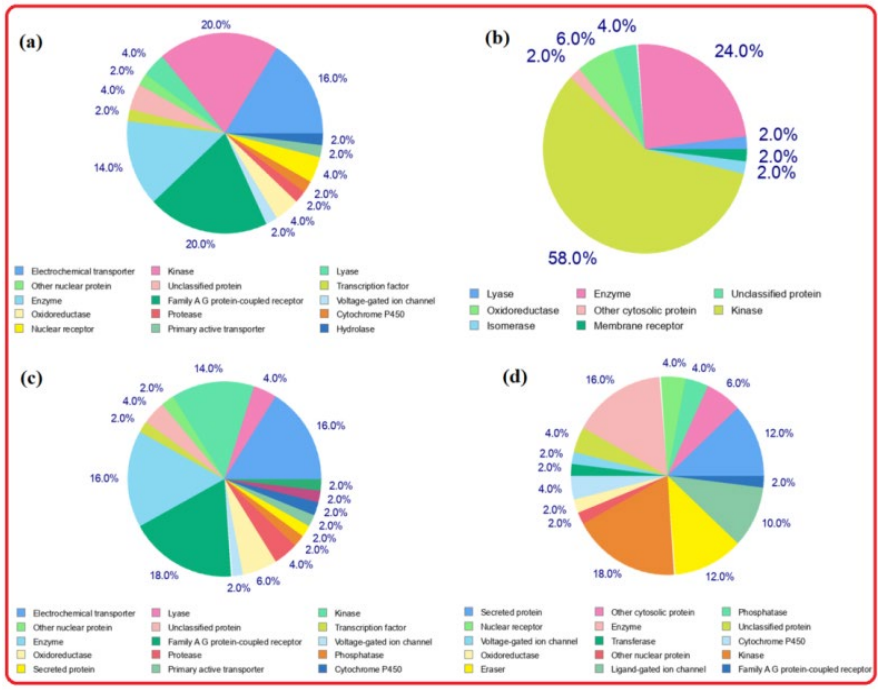

Fig. S31 — Swiss target prediction of synthesized salen type compounds (L^1H_2-L^2H_4)

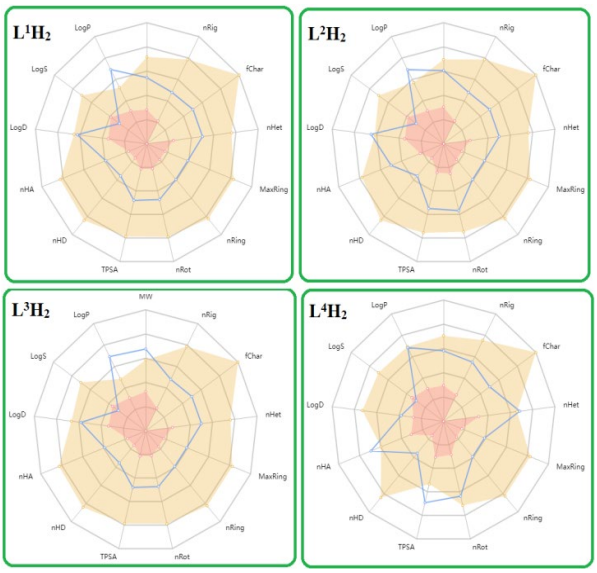

Fig. S32 — The bioavailability radar prediction of synthesized salen type compounds(L^1H_2-L^2H_4)

Table S1 — Bond distances (Å) and bond angles (°) for salen-type compound LH_2

Ligand	Bond lengths (Å)	Bond angles (°)
LH_2	C(1)-C(2) 1.382(8)	C(2)-C(1)-C(6) 119.6(5)
	C(1)-C(6) 1.394(8)	C(2)-C(1)-Br(1) 119.0(4)
	C(1)-Br(1) 1.886(6)	C(6)-C(1)-Br(1) 121.3(4)
	C(2)-C(3) 1.389(7)	C(1)-C(2)-C(3) 120.2(5)
	C(2)-H(2) 0.9400	C(1)-C(2)-H(2) 119.9
	C(3)-C(4) 1.410(7)	C(3)-C(2)-H(2) 119.9
	C(3)-C(7) 1.471(7)	C(2)-C(3)-C(4) 119.8(5)
	C(4)-O(1) 1.341(7)	C(2)-C(3)-C(7) 119.8(5)
	C(4)-C(5) 1.396(7)	C(4)-C(3)-C(7) 120.4(5)
	C(5)-C(6) 1.355(9)	O(1)-C(4)-C(5) 119.6(5)
	C(5)-H(5) 0.9400	O(1)-C(4)-C(3)
	C(6)-H(6) 0.9400	121.7(5)
	C(7)-N(1)	C(5)-C(4)-C(3)

	1.266(8) C(7)-H(7) 0.9400 C(8)-N(1) 1.466(7) C(8)-C(8)#1 1.488(11) C(8)-H(8A) 0.9800 C(8)-H(8B) 0.9800 O(1)-H(1) 0.8300	118.7(5) C(6)-C(5)-C(4) 120.9(5) C(6)-C(5)-H(5) 119.5 C(4)-C(5)-H(5) 119.5 C(5)-C(6)-C(1) 120.8(5) C(5)-C(6)-H(6) 119.6 C(1)-C(6)-H(6) 119.6 N(1)-C(7)-C(3) 122.7(5) N(1)-C(7)-H(7) 118.7 C(3)-C(7)-H(7) 118.7 N(1)-C(8)-C(8)#1 110.1(6) N(1)-C(8)-H(8A) 109.6 C(8)#1-C(8)-H(8A) 109.6 N(1)-C(8)-H(8B) 109.6 C(8)#1-C(8)-H(8B) 109.6 H(8A)-C(8)-H(8B) 108.1 C(7)-N(1)-C(8) 118.3(5) C(4)-O(1)-H(1) 109.5
Symmetry transformations used to generate equivalent atoms: #1 -x+1,-y+1,-z+2		

Table S2 — Hydrogen bonds for salen type compoundLH_2 [Å and °]				
D-H...A	d(D-H)	d(H...A)	d(D...A)	<(DHA)
C(8)-H(8B)...N(1)#2	0.98	2.63	3.583(9)	165.1
O(1)-H(1)...N(1)	0.83	1.87	2.609(6)	147.8
C(8)-H(8B)...N(1)#2	0.98	2.63	3.583(9)	165.1
Symmetry transformations used to generate equivalent atoms: #1 – x+1,-y+1,-z+2 #2 x,-y+1/2, z+1/2				

Table S3 — The Swiss-ADME computed parameters results of synthesized salen type compoundsLH_2-L^4H_2							
Swiss-ADME computed parameter	CQ [a]	HCQ [a]	LH_2	L^1H_2	L^2H_2	L^3H_2	L^4H_2
M.W (150-500g/mol)	285.43	287.40	426.10	406.09	486.15	771.90	448.30
H-acceptors (≤10)	2	3	4	4	6	4	12
H-donors (≤5)	1	2	2	2	2	2	2
Log P (0.7-5.0)	4.15	3.32	4.16	5.24	4.17	5.05	2.26
No. of violation (Rule of 5)	0	0	0	1	0	2	1
TPSA (20-130 $Å^2$)	28.16	48.39	65.18	65.18	83.64	65.18	248.46
Rotatable bonds (<9)	7	7	5	5	7	5	9
Log S(>-6)	-3.95	-3.37	-4.49	-5.66	-4.82	-5.76	-7.34
Fraction Csp^3 (>0.25)	0.5	0.47	0.12	0.12	0.22	0.12	0.12

Table S4 — The physiochemical properties of synthesized salen type compounds (LH_2-L^4H_2)					
Physiochemical Property	LH_2	L^1H_2	L^2H_2	L^3H_2	L^4H_2
Molecular Weight	426.10	4.6.09	486.15	771.90	448.30
Log P	4.541	5.346	4.359	6.534	2.932
Log S	-4.596	-5.314	-5.284	-4.835	-4.591
Log D	3.458	2.803	3.264	2.487	1.481
nHA	4	4	6	4	16
nHD	2	2	2	2	2
TPSA	65.18	65.18	83.64	65.18	237.74
nRot	5	5	7	5	9
nRing	2	2	2	2	2
MaxRing	6	6	6	6	6
nHet	6	8	8	8	16
fChar	0	0	0	0	0
nRig	14	14	14	14	18

Table S5 — Pharmacokinetics properties of the investigated salen-type compounds (LH_2-L^4H_2)					
			Absorption		
Property	LH_2	L^1H_2	L^2H_2	L^3H_2	L^4H_2
Pgp-substrate	0.003	0.927	0.004	0.279	0.867
HIA	0.025	0.002	0.101	0.005	0.02
$F_{20\%}$	0.265	0.265	0.165	0.201	0.004
$F_{30\%}$	0.031	0.997	0.01	0.669	0.001
Caco-2 Permeability	-5.164	-5.328	-5.36	-5.247	-4.927
			Distribution		
PPB	96.45 %	100.6 %	97.56 %	98.52 %	98.39 %
VD	0.983	0.696	0.877	0.629	1.367
BBB Penetration	0.24	0.101	0.131	0.029	0.981
Fu	6.576 %	0.941 %	3.775 %	2.608 %	4.193 %
			Metabolism		
CYP1A2 inhibitor	0.749	0.468	0.816	0.591	0.499
CYP1A2 substrate	0.618	0.847	0.923	0.54	0.093

CYP2C19 inhibitor	0.168	0.077	0.073	0.025	0.302
CYP2C9 inhibitor	0.108	0.167	0.058	0.084	0.531
CYP2D6 inhibitor	0.967	0.757	0.87	0.137	0.084
Excretion					
CL	0.83	1.795	1.045	0.674	0.809
$T_{1/2}$	0.255	0.084	0.59	0.023	0.309
Toxicity					
hERG Blockers	0.016	0.034	0.183	0.118	0.232
H-HT	0.049	0.048	0.084	0.084	0.148
DILI	0.573	0.912	0.616	0.555	0.962
Eye corrosion	0.955	0.004	0.24	0.01	0.003
Respiratory Toxicity	0.843	0.794	0.922	0.909	0.746
Environmental toxicity					
IGC_{50}	5.282	5.406	5.165	6.072	4.623
$LC_{50}FM$	6.214	6.455	6.481	6.833	6.081
$LC_{50}DM$	6.465	6.369	6.776	6.716	5.899
Tox21 pathway					
NR-AR-LBD	0.006	0.031	0.021	0.093	0.566
SR-MMP	0.932	0.97	0.911	0.975	0.994